

## Network modification of phosphate materials by transition metals doping

O. Kostadinova<sup>1\*</sup>, D. Kochnitcharova<sup>1</sup>, E. Lefterova<sup>1</sup>, M. Shipochka<sup>2</sup>, P. Angelov<sup>1</sup>, T. Petkova<sup>1</sup>

<sup>1</sup> Section Solid State Electrolytes, Institute of Electrochemistry and Energy systems "Acad. Evgeni Budevsky", Bulgarian Academy of Sciences, Acad. G. Bonchev Str., bld. 10, 1113 Sofia, Bulgaria

<sup>2</sup> Institute of General and Inorganic Chemistry, Bulgarian Academy of Sciences, "Acad. Georgi Bonchev" Str. bld. 11, 1113 Sofia, Bulgaria

Received November 10, 2017; Accepted December 04, 2017

This work is focused on structural modification of phosphate materials by doping with transition metal oxides. The structure of  $(\text{TiO}_2)_x(\text{V}_2\text{O}_5)_y(\text{P}_2\text{O}_5)_{100-x-y}$  composites is discussed in terms of composition, structural units and valence variations. XRD diffraction, IR and XPS spectroscopic techniques are used to analyze the materials. The addition of  $\text{V}_2\text{O}_5$  and  $\text{TiO}_2$  destroys P-O-P bridge structure, generates mixed P-O-V bonds and non-bridged oxygen atoms leading to the appearance of isolated  $\text{PO}_4^{3-}$  units.

**Keywords:** transition metal oxide, structural study, IR, XPS

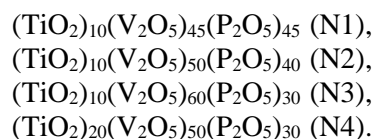
### INTRODUCTION

The need of urgent development of alternative energy sources continuously increases. The solid oxide fuel cells (SOFCs) are a promising response since they can operate reversibly, storing excess of renewable electricity in electrolysis mode, and then converting the fuel back to electricity in fuel cell mode [1]. The most favourable approach in SOFCs optimization is to lower the operating temperatures (200-600 °C). Composite materials with charge imbalance caused by the cation non-stoichiometry compensated by protons (cation off-stoichiometric materials) are among the promising candidates for SOFC electrolytes. The non-stoichiometry is a typical behaviour of the transition metals that can influence the materials properties. With incorporation of transition metal ions, one may introduce non-stoichiometry and create new pathways for proton mobility due to structure reformation [2, 3]. In this respect, the phosphate materials like phosphate glasses, metal pyrophosphates and metal phosphates with NASICON type structure are an interesting subject of scientific work [4-6].

The present study discusses structural modification of  $(\text{TiO}_2)_x(\text{V}_2\text{O}_5)_y(\text{P}_2\text{O}_5)_{100-x-y}$  composites with  $x = 10, 20$  mol % and  $y = 45, 50, 60$  mol % after doping with transition metal.

### EXPERIMENTAL

Bulk samples from  $(\text{TiO}_2)_x(\text{V}_2\text{O}_5)_y(\text{P}_2\text{O}_5)_{100-x-y}$  system were synthesized by melt quenching method. The initial compounds of  $\text{TiO}_2$  and  $\text{V}_2\text{O}_5$  powders and orthophosphoric acid ( $\text{H}_3\text{PO}_4$ ) were homogenized and melted at 1100 °C to obtain samples with compositions:



The structure of the samples was studied by X-ray diffractometer Philips APD-15 using  $\text{CuK}\alpha$  radiation. The IR spectra are recorded by FTIR spectrometer VARIAN 660-IR in the frequency range between 400 - 1400  $\text{cm}^{-1}$  with a resolution of 2  $\text{cm}^{-1}$ . X-ray photoelectron spectroscopy (XPS) measurements were carried out by spectrometer VG ESCALAB II using  $\text{AlK}\alpha$  radiation with energy of 1486.6 eV. The binding energies were determined with an accuracy of  $\pm 0.1$  eV utilizing the  $\text{C}_{1s}$  line at 285.0 eV (from adventitious carbon) as a reference.

### RESULTS AND DISCUSSIONS

#### Structural background

The studied materials are composed of three oxides: vanadium, titanium and phosphorus oxides, connected and forming various groups and units.

The phosphate atoms usually form a network consisting of  $\text{PO}_4$  units linked with neighbouring  $\text{PO}_4$  tetrahedra through one-, two- or three P-O-P bridges (Bridging Oxygen BO), denoted as  $\text{Q}^i$ , where  $i$  is the number of the BO ( $n = 0, 1, 2$  or  $3$ ) [7]. Linkage by two BO ( $\text{Q}^2$  units) can be considered as  $\text{PO}_2^-$  middle groups in phosphate chains, while ( $\text{Q}^1$ ) corresponds to  $\text{PO}_3^{2-}$  terminal units.  $\text{Q}^0$  represents an isolated  $\text{PO}_4^{3-}$  tetrahedron known as orthophosphate unit. The vitreous  $\text{P}_2\text{O}_5$  consists of  $\text{Q}^3$  phosphate tetrahedra that form a three dimensional network. The addition of metal oxides results in "depolymerisation" of this network due to breaking of P-O-P bonds and

\* To whom all correspondence should be sent.  
E-mail: [ofeliya.kostadinova@iees.bas.bg](mailto:ofeliya.kostadinova@iees.bas.bg)

creation of negatively charged non-bridging oxygen (NBO). The  $Q^i$  species change according to Kirkpatrick and Brow model [7, 8] in consecution  $Q^3 \rightarrow Q^2 \rightarrow Q^1 \rightarrow Q^0$  with increasing of the amount of modifying oxide.

The vanadium atoms could be present in different oxygen environments forming various types of polyhedra as  $VO_6$  octahedra,  $VO_5$  groups (square pyramids or trigonal bi-pyramids) and  $VO_4$  tetrahedra in the crystalline and amorphous vanadates [9-12]. In vanadate-phosphate systems mixed units are formed composed of  $VO_x$  and  $PO_4$  polyhedra [12].

The  $TiO_2$  in all polymorph forms is built from  $TiO_6$  octahedra [13].  $TiO_6$  is the main structural unit in the titanium-phosphates as pyrophosphates [14], and NASICON (Na Super Ionic Conductor) like phosphates [15]. In the phosphate glasses Ti atoms are in six-, five- or fourfold coordination [16-18].

#### X-ray Diffraction

The broad halo in XRD patterns reveals the amorphous character of samples N1 and N2 with higher phosphate content (Fig. 1). The samples N3 and N4 are glassy-crystalline as defined from the diffraction peaks and the halo on diffractograms. The higher  $TiO_2$  content (20 mol.%) is accountable for the appearance of pure rutile phase observed in the sample N4. An empty NASICON-type crystal structure was identified for crystalline part of sample N3 -  $(TiO_2)_{10}(V_2O_5)_{60}(P_2O_5)_{30}$  as described in previous work [19]. The structural formula of NASICON-type vanadyl (V) titanium(IV) phosphate proposed by S. Titlbach et. al. [20] is  $(V^{IV}O)Ti^{IV}_6(PO_4)_9$ .

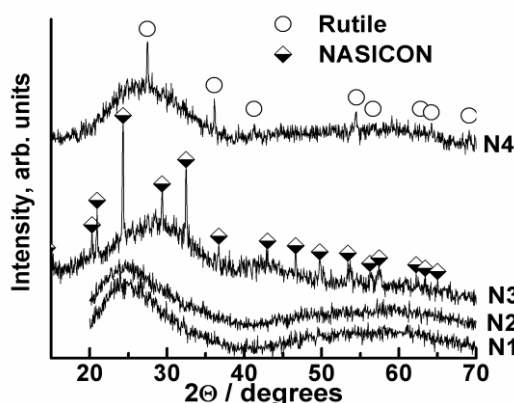


Fig. 1. XRD patterns of samples from  $(TiO_2)_x(V_2O_5)_y(P_2O_5)_{100-x-y}$  system.

#### Infrared study

The infrared spectra of  $(TiO_2)_x(V_2O_5)_y(P_2O_5)_{100-x-y}$  samples are presented in fig. 2. The absorption above  $1200\text{ cm}^{-1}$  and the weak band at  $1180\text{ cm}^{-1}$  on the spectrum of sample N1 are connected with asymmetric and symmetric

stretching of  $PO_2^-$  ( $Q^2$ ) middle groups in phosphate chains [21]. The absence of a pronounced absorption peak at  $\sim 1250\text{ cm}^{-1}$  however demonstrates the formation of short chains. The bands at  $1130\text{ cm}^{-1}$  and  $1064\text{ cm}^{-1}$  are due to vibrations of  $PO^-$  in  $PO_3^{2-}$  ( $Q^1$ ) terminal groups in the phosphate chains and pyrophosphate units  $P_2O_7^{4-}$ , respectively [22, 23]. The P-O-P bridges absorb at  $\nu_{as} \sim 900\text{ cm}^{-1}$  and  $\nu_s \sim 740\text{ cm}^{-1}$ . The bands at the  $940\text{ cm}^{-1}$  and  $870\text{-}850\text{ cm}^{-1}$  are due to the symmetric and anti-symmetric stretching vibration of the  $VO_2$  groups in the  $VO_4$ -polyhedra [9, 10]. The absorption at  $1010\text{ cm}^{-1}$  might arise from stretching vibration of  $V=O$  vanadyl bond in  $VO_5$ -groups or/and normal mode of  $PO_4^{3-}$  ( $Q^0$ ) isolated phosphate groups [24]. In the glass N1 probability to detect  $PO_4^{3-}$  unit is small, therefore more likely  $VO_5$  and  $VO_4$  units are present. With the increasing of the  $V_2O_5$  content the absorption band at  $\sim 940\text{ cm}^{-1}$  disappeared and  $VO_4$  units is not registered on IR spectrum of glass N2. The spectra of N3 and N4 are comparable: the absorption above  $\sim 1200\text{ cm}^{-1}$ , related to the  $PO_2^-$  phosphate groups, disappears and the band at  $900\text{ cm}^{-1}$  shifts to lower ( $860\text{ cm}^{-1}$ ) wavenumber due to mixed P-O-V bridge formation. This indicates that no phosphate chains in these samples exist and they are built of  $Q^1$  and  $Q^0$  species.

The IR spectrum of the glassy-crystalline sample N3 is similar to this of crystalline  $NaTi_2(PO_4)_3$  [25,26] NASICON structure. The structure consists of  $TiO_6$  octahedra which share corners with six  $PO_4$  tetrahedra while each  $PO_4$  tetrahedron is connected by the corner with four  $TiO_6$  octahedra [15]. As a result, isolated phosphate group  $PO_4^{3-}$  ( $Q^0$ ), located at  $\sim 996\text{ cm}^{-1}$  and bending at  $576\text{ cm}^{-1}$ , as well as normal vibration of  $TiO_6$  octahedra  $\sim 640\text{ cm}^{-1}$  are identified in N3 spectrum. The band at  $1020\text{ cm}^{-1}$  is due to  $V=O$  in  $VO_5$  trigonal bipyramid.

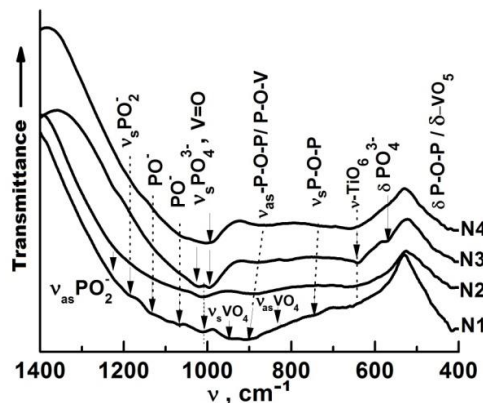


Fig. 2. Infrared spectra of samples  $(TiO_2)_x(V_2O_5)_y(P_2O_5)_{100-x-y}$  system

The formation of TiO<sub>2</sub> Rutile phase leads to the higher concentration of P<sub>2</sub>O<sub>5</sub> in amorphous matrix, which reflect on the IR spectrum of sample N4 as shoulder located at 1060 cm<sup>-1</sup> because of the appearance of additional PO<sub>3</sub><sup>2-</sup> (Q<sup>1</sup>) groups.

The bands in the 400 – 500 cm<sup>-1</sup> range are due to the lattice vibrations in vanadium oxide network and deformation of PO<sub>4</sub> units.

#### X-ray Photoelectron spectroscopy investigation

The XPS spectra shown in Fig 3 (a-d) validate the existence of different structure units. The broad P2p high resolution spectra are deconvoluted in three P2p<sub>3/2</sub>-P2p<sub>1/2</sub> doublets which correspond to Q<sup>0</sup> tetrahedra (PO<sub>4</sub><sup>3-</sup>) at ~132.5 eV, Q<sup>1</sup> (PO<sub>3</sub><sup>2-</sup>) at ~133.5 eV and (PO<sub>2</sub>)<sup>-</sup> Q<sup>2</sup> with binding energy (BE) around 134.5 eV [27, 28]. The dominance of pyrophosphate groups P<sub>2</sub>O<sub>7</sub><sup>4-</sup> is clearly visible. The number of isolated PO<sub>4</sub><sup>3-</sup> phosphate group increases when the P<sub>2</sub>O<sub>5</sub> content decreases (grow of component Q<sup>0</sup>) whereas more PO<sub>2</sub><sup>-</sup> units (Q<sup>2</sup>) are detected at higher phosphate content.

O1s peak was deconvoluted in three components (Fig 3b): O1 with BE around 259-530.5 eV correspond to non-bridging oxygen (NBO) which forms oxygen bonds with titanium or vanadium and V-O-V bridges; O2 peak with BE=531-532 eV is assigned to mixed bridging bonds V-O-P and component O3 with BE of 533-534 eV associated with bridged oxygen in P-O-P bond or oxygen from adsorbed water [28].

The peak position of Vp<sub>3/2</sub> at ~517.6 eV (fig.3c) is evidence for predominantly V<sup>5+</sup> valence of vanadium. The deconvolution with two components reveals weak asymmetry towards the lower energies due to the presence of V<sup>4+</sup> with BE ≈ 516.5 eV.

Ti2p spectra on fig. 3(d) indicates the existence of Ti<sup>4+</sup> valence state with BE(Ti2p<sub>3/2</sub>) ≈ 459.3 eV in the crystalline samples corresponding to Anatase/Rutile BE [29]. The BE of Ti in the glassy samples is shifted to higher values at 459.85 eV.

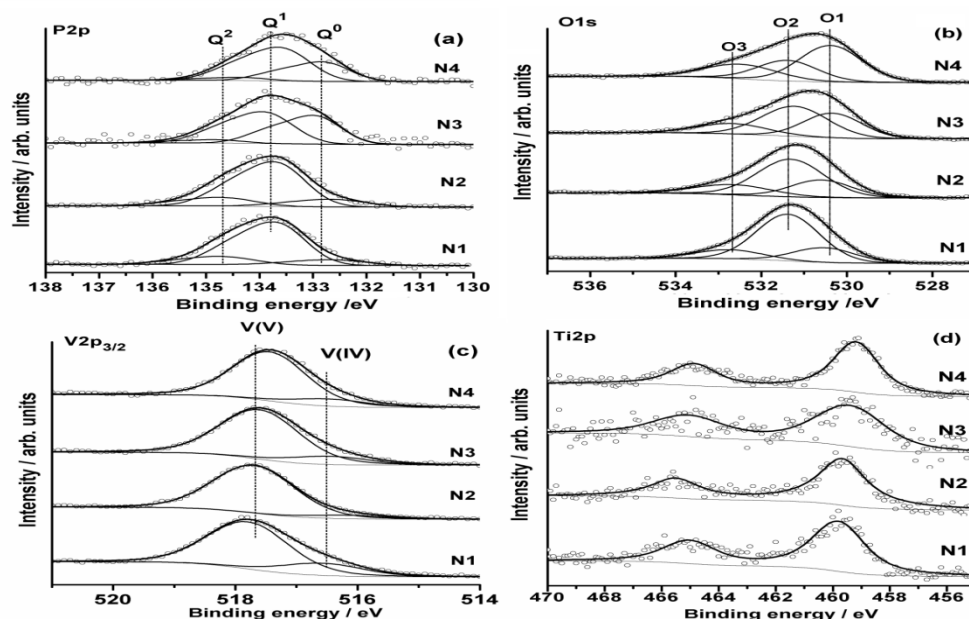


**Fig. 3.** High resolution X-ray photoelectron spectra of the (TiO<sub>2</sub>)<sub>x</sub>(V<sub>2</sub>O<sub>5</sub>)<sub>y</sub>(P<sub>2</sub>O<sub>5</sub>)<sub>100-x-y</sub> samples: (a) P2p ; (b) O1s; (c) V2p<sub>1/2</sub>; (d) Ti2p.

FTIR and XPS investigations show that pyrophosphate (P<sub>2</sub>O<sub>7</sub>)<sup>4-</sup> units are the major group in the samples under study. The units, however, are partially displaced by isolated PO<sub>4</sub><sup>3-</sup> when the phosphorus content decreases or by PO<sub>2</sub><sup>-</sup> units when the phosphate content grows.

The samples N3 and N4 are based on both: Q<sup>1</sup> with a two PO<sub>3</sub><sup>2-</sup> tetrahedra connected in pyrophosphate units and Q<sup>0</sup>, i.e. isolated PO<sub>4</sub><sup>3-</sup> tetrahedra. The vanadium pentoxide plays role of the second glass former. Addition of V<sub>2</sub>O<sub>5</sub> and/or

TiO<sub>2</sub> leads to destroying P-O-P bridge structure introducing mixed P-O-V bridges and new NBOs. The titanium atoms possess stable fourth valence and octahedral coordination in all samples.

#### CONCLUSIONS

The study of materials from (TiO<sub>2</sub>)<sub>x</sub>(V<sub>2</sub>O<sub>5</sub>)<sub>y</sub>(P<sub>2</sub>O<sub>5</sub>)<sub>100-x-y</sub> system reveals that the structure is characterized by different oxygen environment. The addition of V<sub>2</sub>O<sub>5</sub> and TiO<sub>2</sub> leads to destroying P-O-P bridge structure introducing mixed P-O-V bridges and new NBOs. The

pyrophosphate ( $P_2O_7^{4-}$ ) groups are the main structural units in the samples partially displaced by isolated  $PO_4^{3-}$  groups when the  $V_2O_5$  and/or  $TiO_2$  content increases or by  $PO_2^-$  units when the content of the transition metals decreases. The glass-crystalline samples with NASICON or Rutile type-structure possess lower  $P_2O_5$  content.

The vanadium exist in two valence states  $V^{5+}$  and  $V^{4+}$ . The presence of  $VO_5$  groups and  $TiO_6$ -octahedra is typical to all studied samples.

**Acknowledgment:** The research leading to these results has received funding from Bulgarian NSF under grant No E02/3/2014.

#### REFERENCES

1. D. Vladikova, Z. Stoynov, G. Raikova, A. Thorel, A. Chesnaud, J. Abreu, M. Viviani, A. Barbucci, S. Presto, P. Carpanese, *Electrochim. Acta*, **56**, 7955 (2011).
2. R. V. Barde, S. A. Waghuley, *J. Advanced Ceramics*, **2**, 246 (2013).
3. B. Zhu, *Solid State Ionics*, **145**, 371 (2001).
4. Y. Daiko, *Journal of the Ceramic Society of Japan (JCS-Japan)*, **121**, 539 (2013)
5. Y. Jin, Y. Shen and Takashi Hibino, *Mater. Chem.*, **20**, 6214 (2010).
6. M.A. Moshareva, S.A. Novikova, A.B. Yaroslavtsev, *Inorg. Mater.*, **52**, 1283 (2016).
7. R. K. Brow, *J. Non-Cryst. Solids*, **263&264**, 1 (2000).
8. R.K. Brow, C.A. Click, T.M. Alam, *J. Non-Cryst. Solids*, **274**, 9 (2000).
9. V.Dimitrov, *J. Non-Cryst. Solids*, **192&193**, 183 (1995).
10. Y. Dimitriev, V. Dimitrov, M. Arnaudov, and D. Topalov, *J. Non-Cryst. Solids*, **57**, 147 (1983).
11. M. Willinger, N. Pinna, D. S. Su, R. Schlögl, *Physical Review B*, **69**, 155114 (2004).
12. S. Boudin, A. Guesdon, A. Leclaire, M.-M. Borel, *Int. J. Inorg. Materials*, **2**, 561 (2000).
13. M. Matsui, M. Akaogi, *Molecular Simulation*, **6**, 239 (1991).
14. S. T. Norberg, G. È. Svensson and J. È. Albertsson, *Acta Cryst.*, **C57**, 225 (2001).
15. S. Benmokhtar, A. El Jazouli, A. Aatiq, J.P. Chaminade, P. Gravereau, A. Wattiaux, L. Fourne`s, J.C. Grenier, *J. Solid St. Chem.*, **180**, 2004 (2007).
16. A. Tang, T. Hashimoto, T. Nishida, H. Nasu, K. Kamiya, *Journal of Ceramic Society of Japan*, **112**, 496 (2004).
17. B. Tiwari, A. Dixit, G. P. Kothiyal, M. Pandey, S. K. Deb, *BARC Newsletter*, **285**, 167 (2007).
18. S. Lee, H. Maeda, A. Obata, K. Ueda, T. Narushima, T. Kasuga, *J. Non-Cryst. Solids*, **426**, 35 (2015).
19. D. V. Blaskova-Kochnitcharova, T. Petkova, L. Fachikov, E. Lefterova, I. Kanazirski, P. Angelov, S. Vassilev, *Bulg. Chem. Commun.*, **45:A**, 159 (2013).
20. S. Titlbach, W. Hoffbauer, R. Glaum, *J. Solid State Chem.*, **196**, 565 (2012).
21. L. L. Velli, C. P. E. Varsamis, E. I. Kamitsos, D. Möncke & D. Ehrt, *Phys. Chem. Glasses*, **46**, 178 (2005).
22. A. Shaim, M. Et-tabirou, *Materials Chemistry and Physics*, **80**, 63 (2003).
23. K. Nakamoto, *Infrared and Raman Spectra of Inorganic and Coordination Compounds: Part A: Theory and Applications in Inorganic Chemistry*, Sixth Edition John Wiley & Sons, Inc., 2009
24. H-K Roh, M-S Kim, K. Chung, M. Ulaganathan, V. Aravindan, S. Madhavi, K. Roh, K-B Kim, *Journal of Materials Chemistry A*, **5**, 17506 (2017).
25. P. Tarte, A. Rulmont & C. Merckaert-Ansay, *Spectrochimica Acta*, **42A**, 1009 (1986).
26. R. Gresch, W. Muller-Warmuth, H. Dutz, *J. Non-Cryst. Solids*, **34**, 127 (1979).
27. A. V. Naumkin, A. Kraut-Vass, S. W. Gaarenstroom, C. J. Powell, NIST Standard Reference Database 20, Version 4.1 (2013), <http://srdata.nist.gov/xps>
28. A. Majjane, A. Chahine, M. Et-tabirou, B. Echchahed, T. Do, P. Mc Breen, *Mater. Chem. Phys.*, **143**, 779 (2014).
29. U. Diebold, T. E. Madey, *Surf. Sci. Spectra*, **4**, 227 (1996).

## МОДИФИЦИРАНЕ НА МРЕЖАТА НА ФОСФАТНИ МАТЕРИАЛИ ЧРЕЗ ДОТИРАНЕ С ПРЕХОДНИ МЕТАЛИ

О. Костадинова<sup>1</sup>, Д. Кошничарова<sup>1,2</sup>, Е. Лефтерова<sup>1</sup>, М. Шипочка<sup>3</sup>, П. Ангелов<sup>1</sup>, Т. Петкова<sup>1</sup>

<sup>1</sup>*Институт по електрохимия и енергийни системи "Акад. Евгени Будевски", Българска академия на науките, ул. "Акад. Г. Бончев", бл. 10, 1113 София, България*

<sup>2</sup>*Химикотехнологичен и металургичен университет, бул. "Климент Охридски" 8, 1756 София, България*

<sup>3</sup>*Институт по обща и неорганична химия, Българска академия на науките, ул. "Акад. Георги Бончев" бул. 11, 1113 София, България*

Постъпила на 10 ноември, 2017 г.; приета на 04 декември, 2017 г.

(Резюме)

Тази работа се фокусира върху изследването на структурните промени на фосфатните материали при дотиране с оксиди на преходните метали. Структурата на новите композити  $(\text{TiO}_2)_x(\text{V}_2\text{O}_5)_y(\text{P}_2\text{O}_5)_{100-x-y}$  се разглежда по отношение на състава, структурните единици и валентността. За анализ на материалите се използват Ренгенова дифракция, ИЧ и фотоелектронна спектроскопия. Добавянето на  $\text{V}_2\text{O}_5$  и  $\text{TiO}_2$  разрушава Р-О-Р мостовата структура и води до образуване на смесени и немостови кислородни връзки, както и до появата на изолирани  $\text{PO}_4^{3-}$  единици. При високо съдържание на преходните метали са получени стъклокристални образци.

**Ключови думи:** оксиди на преходни метали, структурни изследвания, IR, XPS